Evaluation of a structural epoxy adhesive for timber-glass bonds under shear loading and different environmental conditions

Žiga Unuk, Andrej Ivanič, Vesna Žegarac Leskovar, Miroslav Premrov, Samo Lubej*

University of Maribor, Faculty of Civil Engineering, Transportation Engineering and Architecture, Smetanova Ulica 17, 2000 Maribor, Slovenia

ABSTRACT

This article presents a study of timber-glass adhesive joints. It examines the shear specimen and shear tools preparation process and the evaluation of the results backed up with an overview of existing similar studies. The chosen adhesive was a cold-curing two-component structural bonding epoxy resin (Mapei Adesilex PG1). The shear tests were performed under different temperatures and the timber samples had different moisture contents. A simple shear test tool was designed and was clamped into a universal testing machine for the shear test. The force and crosshead displacement values from the universal testing machine were used for evaluating the results. The environmental conditions of 20 °C and 5% timber moisture content resulted in the highest average shear strength obtained from the shear tests of the analysed joints (9.89 MPa), whereas the environmental conditions of 50 °C and 20% timber moisture content resulted in the lowest average shear strength (3.42 MPa). It was found that the joint strength is dependent on the environmental temperature *and* timber moisture content. Moreover, the shear specimen load-displacement behaviour at the environmental temperature of 50 °C was linear and nonlinear – depending on the timber moisture content. The most frequent failure type was timber failure. Additionally, a nonlinear contact finite element analysis was performed to demonstrate the additional shear specimen rotation due to the clearance between the shear specimen and shear tools. This impact was evaluated regarding the stress distribution in the bond line. The evaluated epoxy resin adhesive was proved to be suitable for timber-glass bonds.

1. Introduction

Composite timber-glass structures or structural components have become an important and acknowledged segment of modern building construction. For a presentation of the timber-glass structures field progress in the last years see for example Žegarac Leskovar and Premrov's work [1] or Blyberg's et al. study [2]. Although glass is a transparent material with relatively high strength (compared to timber), it has a negative feature of brittle behaviour. However, when glass is combined with timber, the resulting structure can have some ductility and is, therefore, safer than a similar structure consisting solely of glass. An example of a ductile timber-glass structural element are timber-glass composite beams (see for example Rodacki's et al. study [3] where all investigated timber-glass beams failed in a ductile manner). There are several examples of timber-glass composites, which can be roughly arranged into three groups: besides the aforementioned timber-glass beams (see for example Premrov et al. [4]) there are also timber-glass wall panels (see Fig. 1 and Ber et al. [5]) and timber-glass

floor/roof panels (see for example Cruz and Pequeno [6]).

As glass is a brittle material, one of the most important properties of the adhesives is their stiffness. A lower adhesive stiffness ensures more evenly distributed stresses at the bonded interface but is usually also an indicator of lower adhesive strength. Different adhesive types have been tested in various studies: from flexible silicone adhesives to semi-rigid adhesives like polyurethane and to rigid adhesives like acrylate and epoxy. Regarding the rigidity/flexibility limit values, the standard BS EN ISO 527-1:2012 can be considered, as it is frequently used for the determination of mechanical properties of adhesives. Adhesives with elastic moduli greater than 700 MPa can be considered rigid, with elastic moduli greater than 70 MPa and less than 700 MPa semi-rigid and with elastic moduli less than 70 MPa flexible. According to Banea et al. [8], thinner adhesive layers are preferred over thicker adhesive layers, due to lesser stress concentrations, however, ductile adhesives might perform better with slightly thicker adhesive layers as the energy can be dissipated more in a greater volume. As ductile adhesives are usually also flexible and vice versa (according to Campilho and da Silva

---

Fig. 1. Timber-glass wall panel static racking test (adopted from Ber et al. [5]) and two-story timber-glass building shaking table test (adopted from Ber et al. [7]).

[9]), the same principle can be considered for flexible adhesives. For composite timber-glass structures, the adhesive shear properties are usually the most important, which is why the majority of the studies include some variations of shear tests. Cruz and Pequeno [10] performed shear tests of bonded timber-glass connections in a way that two timber parts (Douglas fir) were glued to one glass part (tempered glass), resulting in a symmetric shear specimen. Different adhesives (silicone, polyurethane, acrylate, methacrylate, modified silane, polyvinyl butyral) were used under different timber moisture contents and temperatures. It was found that the timber moisture content had a higher influence on the bond than the temperature. Another experimental study of adhesive joints for spruce timber and float glass with adhesives like silicone, acrylate and polyurethane was performed by Blyberg et al. [11]. The specimens were tested under shear and tension, for which special fixtures were developed. Another experimental investigation was carried out by Vallee et al. [12], who performed shear tests with spruce, beech and oak timber. Tempered glass and different adhesives (polyurethanes, acrylates, epoxies and epoxy silane) were used. Before the test, the shear specimens were subjected to simultaneous cyclic variations of temperature and humidity (after the prescribed hardening time). The shear specimens were tested according to the European standard EN 1465:2009. The results indicated an influence of the timber species on the degradation of joint shear strengths due to weathering. Buyuktaskin et al. [13] executed shear and tension tests on small timber-glass specimen bonded with a two-component silicone adhesive. The specimens were subjected to wetting-drying, freezing-thawing, UV effects, acids and high temperature prior testing. Hydrochloric acid and freezing-thawing were shown to be the most important aging agents that decisively impact the properties of the adhesive under shear forces. Nicklisch's work [14] contains probably the most extensive study on the usage of different adhesives (silicone, polyurethane, epoxy silane, acrylate, epoxy) for bonding of glass (float and tempered) to timber (birch, pine). Different approaches were used to test the bonds in shear, from special fixtures to gripping the shear specimens directly – the standard ISO 11003-2 was used as a reference. The temperature and timber moisture contents were also varied. The timber-glass specimens were artificially aged by subjecting them to UV light, detergent solution and sulfur dioxide containing atmosphere. The two-component epoxy adhesive was shown to be resistant to UV light exposure, but on the other hand shortcomings regarding exposure to sulfur dioxide containing atmosphere and the detergent solution were noticed (loss of adhesion to the glass surface). Long term tests were performed and the results indicated that creep effects were negligible for the bond with the cold curing epoxy adhesive. As Vallee et al. [12] already concluded, one aspect of the progress in timber-glass bonding is the transition from using flexible adhesives (like silicones) to semi-rigid adhesives like polyurethane and rigid adhesives (like epoxies). It can also be understood as a process of enlarging the load shared to the glass in a composite structure. For elements exposed to indoor and outdoor

temperature (timber-glass wall elements), the current state of the art is to use semi-rigid adhesives like polyurethane to cope with the different thermal expansions of glass and timber. For elements which are placed indoor (timber-glass beams), where the temperature is somewhat constant or controlled, stiffer adhesives can be used. The advantage of epoxy resins is their resistance to changing environmental loads as pointed out by Vallee et al. [12].

The existing examples of timber-glass composites are all new and individual structural elements. Another possible usage of glass in combination with timber could be the strengthening of an existing timber structure in a way that glass would be used instead of steel, carbon fibre reinforced polymers or glass fibre reinforced polymers. Comparing the characteristic tensile strength parallel to grain of spruce timber with strength class C24 (as defined in the European standard EN 338:2016, which is commonly accepted as an average spruce timber strength class) and the characteristic tensile strength of tempered glass (as defined by the draft European standard prEN 16612:2017), this seems to be an option worthy of testing, as the tempered glass characteristic tensile strength (120 MPa) is much higher than the timber C24 characteristic tensile strength parallel to grain (14 MPa). As a strengthening procedure is basically an attempt to install the additional strengthening element in a way that a considerable amount of the structural load is transferred to it, rigid adhesives are commonly used to maximize the composite action. The purpose of this research is therefore to study the application of a recognized structural repair epoxy resin (a rigid adhesive) for strengthening existing timber structures with tempered glass, resulting in a timber-glass composite and to form a basis for possible future research of such a timber-glass composite usage. Small shear specimens are formed and the shear strength of the bond is experimentally investigated. As existing timber structures can be subjected to varying environmental conditions, the focus of this study is on the combined impact of the timber moisture content (which depends on the air humidity and temperature) and the environment temperature on the shear strength of a bonded timber-glass joint. The chosen shear test method is additionally evaluated with a finite element simulation.

2. Materials and methods

For each combination of environmental conditions (varying moisture and temperature), 7 specimens were tested in shear. The total specimen number was therefore 63 (7 specimens, 3 different temperatures, 3 different moisture contents).

2.1. Testing device

Special shear tools were designed for the shear test (Fig. 2). They were made from structural steel and consisted of two parts. For the shear test, the shear tools were clamped to a Zwick/Roell Z010
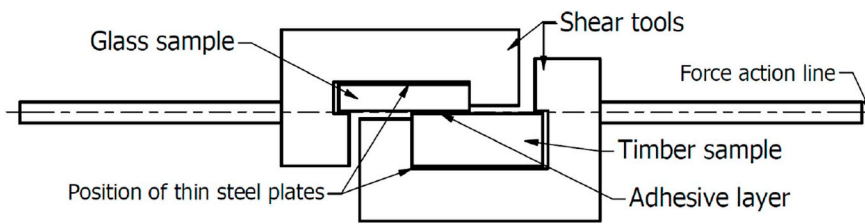
Fig. 2. Shear tools and shear specimen.

universal testing machine. The shear tool parts had different geometries as one part was used for the fixation of the timber sample and the second for fixation of the glass sample. As Serrano [15] showed how friction forces can play a decisive role in the evaluation of shear-strength-predicting capabilities of test specimens for wood–adhesive bonds, it is important to note that due to the specific configuration no contact can be formed between the shear tool part for glass sample fixation and the timber sample. The same holds for the shear tool part for timber sample fixation and the glass sample. The only load transfer between the shear tool parts therefore only happens through the adhesive layer. This means that there are no friction forces between the shear tools and shear specimen that are added to the measured joint force and included in the estimation of the mean shear stress in the adhesive layer. This is an important feature because the adjusting of the measured force due to possible friction forces can easily introduce inaccuracies as the friction forces are difficult to determine and can also vary due to different environmental conditions.

The shear tools and shear specimens were designed in a way that the tolerance for the shear specimen geometry was 1 mm. In this way, possible shear specimen geometry deviations were not a problem in terms of the effortless installation of the shear samples in the testing device. Thin steel plates (with a thickness from 0.1 mm to 1 mm) were used to fill the void between the shear tools and shear specimens (Fig. 2).

Despite the size tolerance positively impacting the installation of the shear specimens into the testing device, the size tolerance made shear specimen rotation possible, which is an unfavourable effect as it results in larger stresses normal to the bonding area plane. The estimated shear specimen rotation was at least 1.5° (estimated on the basis of rigid body rotation – rotation of the shear specimens in the shear tools). However, as all shear specimens were tested in the same way, the effect of the tolerance was equal for all environmental conditions.

The shear specimen and shear tools were also designed in a way that the (tensile) force line of action was parallel to the bonding area and in the mid-plane of the adhesive layer (in the initial state of undeformed geometry).

2.2. Shear specimens

The shear specimens were samples of timber and samples of float glass, glued together with an epoxy resin adhesive (Fig. 3). The bonded area width was 25 mm and the bonded area length was 20 mm. The adhesive layer thickness was 1 mm.

2.2.1. Timber samples

The timber sample thickness was 20 mm, the timber sample width was 25 mm and the timber sample length was 50 mm. The chosen timber sample species was Norway spruce (Picea abies). Special attention was given to providing a bonding area without timber defects like knots or resin pockets (clear wood). The timber samples were sawn in a way that the bonding area plane was oriented in the radial direction of a log. With this orientation, a possible single annual ring deviation and its negative impact on the bonding area was alleviated. The longer side of the timber samples was oriented parallel to the grain, so that the force of the universal testing machine was also acting parallel to the grain. The timber sample surfaces were also smoothed. The
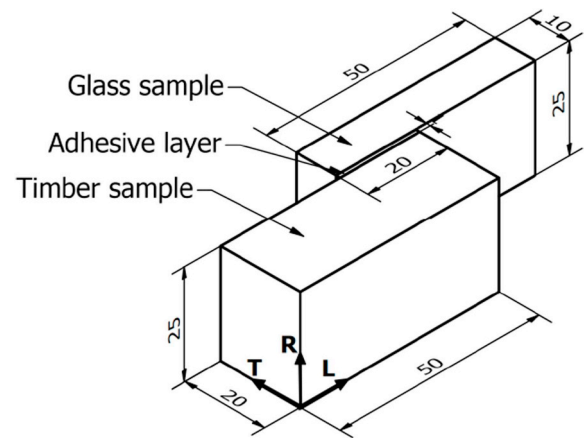

Fig. 3. Shear specimen with indicated timber log axes (L – longitudinal, R – radial, T – tangential).

density was determined with regards to the European standard EN 384:2016 on 9 timber samples. The average density of the timber samples was approximately $444 \frac{kg}{m^3}$ (calculated with the volume at 12% moisture content, with a coefficient of variation of 10%), which is of the size order of the density of Norway spruce clear wood provided by Lavers [16], who gives a value of $417 \frac{kg}{m^3}$ (with a coefficient of variation of 10%). A similar value is given by Dahl and Malo [17], who determined an average density of $398 \frac{kg}{m^3}$ (with a coefficient of variation of 9%). In addition, the elastic modulus in the compression of 6 timber samples was determined (Fig. 4). Additional timber samples with a cross-section of 20 × 25 mm with three different lengths were tested in compression to determine the testing machine compliance ($6.04825 * 10^{-5}$ mm/N). With the knowledge of the machine compliance, the crosshead displacement from the compression test can be used to determine the actual timber sample deformation and elastic modulus. Although, it must be noted that this method is less accurate than optical displacement measurement techniques. The elastic modulus was determined in the interval between 4000 N and 5000 N and its average was approximately 12 GPa with a coefficient of variation of 18%, which is in line with the value (11 GPa) provided by Dahl and Malo [17].

2.2.2. Glass samples

As there is no known difference between the application of adhesives on float, heat strengthened or tempered glass, it was decided to carry out the shear tests with float glass samples. The nominal thickness of the float glass sample was 10 mm, the width was 25 mm and the length was 50 mm. The glass samples were simply cut, without any processing of the edges or surfaces. The bonding area was on the air side of the glass samples, to rule out the possibility of errors due to residues of the tin bed (float glass is produced by floating molten glass on a bed of molten metal, usually tin). Ultraviolet light was used to determine the tin side of the float glass, as the tin side radiates white light when ultraviolet light is directed on it, as a consequence of tin bed residues. However, it is specifically pointed out that the ultraviolet light description is not accurate enough. For example, when an ultraviolet light with a wavelength of 305 nm is used, the shining effect is not
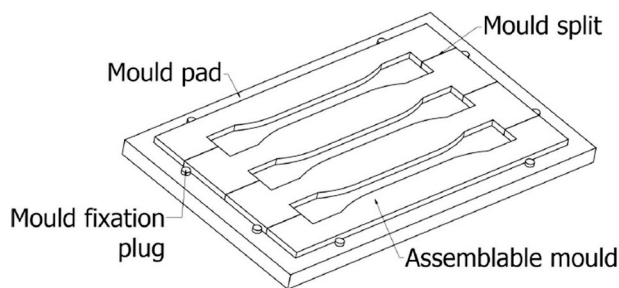
Fig. 4. Timber sample compressive test.

Fig. 5. Epoxy resin specimen mould.

present. Ultraviolet light with a wavelength of 255 nm must be used to observe the described effect, as it is shown by Silvestru et al. [18].

2.2.3. Epoxy resin

The chosen epoxy resin was Adesilex PG1 from the company MAPEI, which is a cold-curing two-component structural bonding epoxy resin of the rapid-setting thixotropic adhesive type. The mixing ratio is 3:1 (component A – resin: component B – hardener). It is a bisphenol-based (bisphenol A and bisphenol F) epoxy adhesive. The hardener (component B) is based on amines and phenols. Fine-grain aggregates (crystalline silica) of a diameter greater than 0.01 mm present 20–25% weight of the adhesive, which is important for limiting the adhesive

Table 2
Adesilex PG1 mechanical properties according to Cerny [20].

Property at 20 °C	Mapei Adesilex PG1
Density [kg/m^3]	1456
E-modulus [MPa]	5716.03
Shear modulus [MPa]	2723.55
Poisson ratio [/]	0.2574
Tensile strength [MPa]	25.13
Shear strength [MPa]	13.70
Strain at failure [%]	0.52
Tensile fracture energy [kJm^{-2}]	1.75
Coefficient of thermal expansion [10^{-6} K^{-1}]	70.46
Water absorption: in 7 days at 25 °C [%w/w]	0.12

shrinkage during curing. According to the producer (MAPEI), the chosen adhesive has the potential for bonding glass elements to timber elements. The complete hardening time of the adhesive is 7 days, as stated by the producer MAPEI [19]. For the characterization of the adhesive properties (tensile elastic modulus and tensile strength) of the chosen epoxy resin, uniaxial tests were performed according to the international standard ISO 527-1:2012. The curing and the tests were performed at a temperature of 20 ± 2 °C and at a relative humidity of 55 ± 5%, which is identical to the conditions specified by the international standard ISO 527-1:2012 (temperature of 23 ± 2 °C, relative humidity of 50 ± 10%). Six specimens were prepared and tested. For the preparation of the specimen, a mould was produced with the process of wire erosion (Fig. 5). The mould could be assembled to simplify the extraction of the epoxy resin specimen. The tests were performed on a Zwick/Roell Z010 with the use of an optical extensometer. The extensometer has an accuracy of 5 μm. The results can be excerpted from Table 1. Cerny [20] determined additional mechanical properties of the Mapei Adesilex PG1 epoxy resin according to the international standard ISO 527-1:2012 (tensile properties) and the standard ASTM D5379 (shear properties) (see Table 2). The average elastic modulus value, determined by tests as a part of this article, was higher than the one determined by Cerny [20]. However, one specimen (tested as a part of this article) resulted in a similar elastic modulus value (5655.15 MPa).

The average strain at failure value and the tensile strength, determined by tests as a part of this article (Fig. 6), were slightly lower than the values determined by Cerny [20]. It can be concluded that the values provided by Cerny [20] are at least nearly in the standard deviation ranges of the tests performed as a part of this article, although details about the number of test specimens are not provided for the study performed by Cerny [20]. It is possible that the differences arose from different curing conditions, as the international standard ISO 527-1:2012 defines relatively large intervals for the specified curing and test conditions.

From the results of the uniaxial tests, the data provided by Cerny [20] and the data found in the producer's documents MAPEI [19], it can be concluded that (at least at a temperature of 20 °C) the epoxy resin outperforms the timber samples in terms of the mechanical properties (tensile, compressive, shear strength, etc.).

2.3. Environmental conditions

The environmental conditions were different temperatures during the shear tests and different moisture contents of the timber samples.
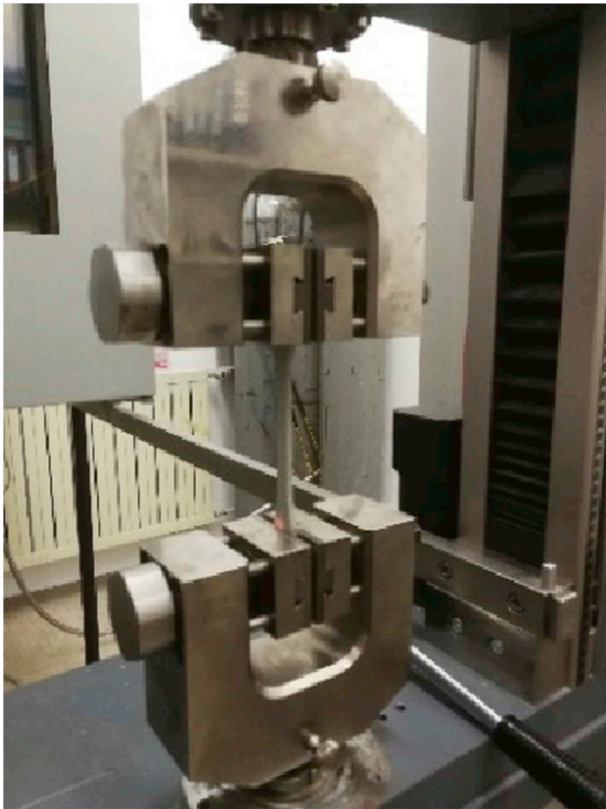
Table 1
Results of the Adesilex PG1 epoxy resin uniaxial tests.

	E-Modulus [MPa]	σ – Tensile strength [MPa]	Strain at failure [%]
	7109.37	24.89	0.37
Standard deviance [MPa]	1014.75	3.50	0.13
Coefficient of variation [%]	14.27	14.06	36.06

Fig. 6. Epoxy resin tensile test.

2.3.1. Test temperature

To simulate different environmental temperatures, the shear tests were performed at 3 different temperatures: -5 °C, $+20 \pm 2$ °C, $+50$ °C. The shear tests were performed inside a temperature chamber. The temperature of -5 °C was reached in approximately 7 min and the temperature of 50 °C in approximately 4 min. The temperature level of $+20 \pm 2$ °C presents the laboratory conditions.

2.3.2. Timber moisture content – epoxy bond curing conditions

As the timber moisture content depends on the air humidity and temperature of the specific environment, existing timber structures can have different moisture contents (usually between 5% and 20% or even more). To examine the effect of the timber moisture content on the joint strength, the timber samples had 3 different levels of moisture content. The planned moisture contents (u) were 5%, 10% and 20%, although there were some deviations between the actual moisture contents and the planned moisture contents. These timber moisture contents correspond to the service classes 1 (u < 12%) and 2 (u < 20%) as defined in the European standard EN 1995-1-1:2004 and cover the vast majority of timber structures at moderate conditions.

The 5% moisture content of the timber samples was reached by drying the timber samples in a drying chamber. The drying was performed in accordance with the European standard EN 13183:2002. The drying temperature was 103 °C. After the sample weight difference was less than 0.1% in an interval of 2 h, the sample was said to be dry. Directly after drying, the timber samples were glued to produce the shear specimens. The shear specimens were then left at the laboratory conditions of $+20 \pm 2$ °C and relative air humidity of 55 ± 5% for 24 h. After 24 h (when the shear specimens could be moved without affecting the specimen geometry), the shear specimens were placed in a desiccator with silica gel for 7 days, to lower the timber sample moisture content again. During this procedure, the moisture content was controlled with the help of 3 control timber samples. 24 h after the bonding procedure, the moisture content of the control samples was

between 6.95% and 8.16% (average 7.64% and standard deviance 0.62%), and after 7 days in the desiccator, the moisture contents were between 4.58% and 4.96% (average 4.78% and standard deviance 0.19%).

The 10% moisture content of the timber samples was reached simply by storing the timber samples at laboratory conditions. Again, control timber samples were used to determine the relative moisture content, which was between 9.24% and 10.98% (average 10.06% and standard deviance 0.87%).

The 20% moisture content of the timber samples was reached by storing the timber samples in a humidity chamber at a temperature of $+20 \pm 2$ °C and relative air humidity of 98 ± 2%. The timber samples were glued right after taking them from the humidity chamber. The shear specimens were then left at laboratory conditions for 24 h. After 24 h (when the shear specimens could be moved without affecting the specimen geometry), the shear specimens were again stored in the high humidity chamber for 7 days, to increase the timber sample moisture content again. During this procedure, the moisture content was controlled with the help of 3 control timber samples. Right before the bonding procedure, the control timber sample moisture contents were between 20.85% and 21.06% (average 20.95% and standard deviance 0.11%). 24 h after the bonding procedure, the moisture content of the control timber samples was between 16.96% and 17.16% (average 17.09% and standard deviance 0.11%), and after 7 days in the high humidity chamber, the control timber sample moisture contents were between 20.61% and 20.78% (average 20.69% and standard deviance 0.09%).

It should be noted that the described conditions for achieving the specific timber moisture content also present the epoxy bond curing conditions. The moisture contents of the glass samples and the epoxy resin layers were not controlled but is clear that the different humidity conditions (during the 7-day period after the glass samples were bonded to the timber samples with the epoxy resin) also affected the final adhesive bond properties. To conclude, the curing of the epoxy bonds was performed at the temperature of $+20 \pm 2$ °C and at three different relative humidity conditions (as described in the previous paragraphs).

2.4. Shear test procedure and measuring method

The timber sample part was held in place while the glass sample part was pushed in the direction of the upper universal testing machine piston (Fig. 7). The displacement rate was 1 mm/min and the preload was 30 N. As the shear tools were clamped into the universal testing machine, the test load was controlled by the displacement rates of the loading pistons, whose movement was used to measure the displacements. Additional devices (extensometer) measuring the displacements and determining the true strains were not applied as the interest of the study was strength-related.

3. Results and discussion

The obtained results gave insight into the impact of (timber) moisture content and temperature on the shear strength of timber-glass joints. Although the average shear stresses do not display the reality in the joints in terms of the stress distribution, they were evaluated in this study as they offer the possibility to compare the results of different studies. Therefore, whenever shear strength is mentioned in this article, the average shear stress is meant, which was calculated by dividing the maximum test load by the bonding area.

3.1. Shear strength

The shear strengths observed during the shear tests under different environmental conditions are presented in Table 3. The highest average shear strength (9.89 MPa) was obtained at the test temperature of 20 ± 2 °C and with timber samples with 5% moisture content. An
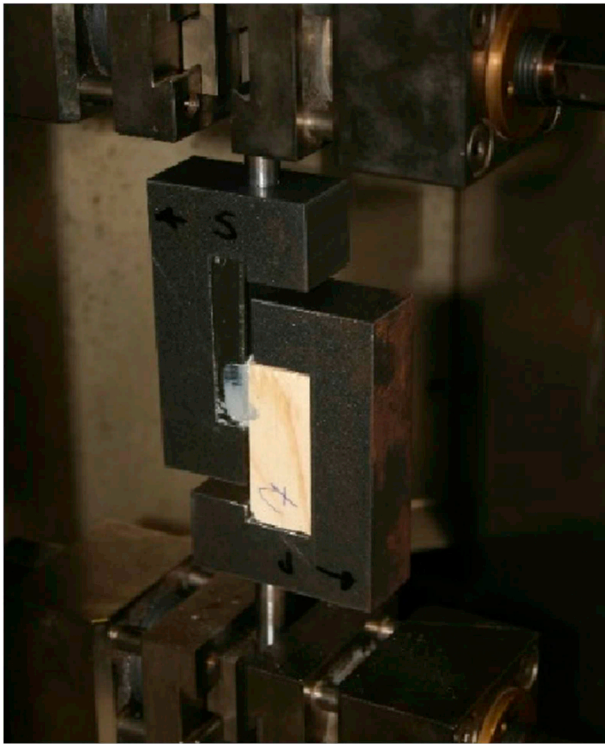
Fig. 7. Testing device.

Table 3
Shear specimen average shear strengths (τ), standard deviations (s) and coefficients of variation (CV) for different test temperatures and timber moisture contents.

				T [°C]		
				−5	20	50
u [%]	5	τ	[MPa]	3.63	9.89	6.21
		s	[MPa]	1.19	1.64	1.38
		CV	[%]	33	17	22
	10	τ	[MPa]	9.84	7.50	5.44
		s	[MPa]	1.99	3.31	1.85
		CV	[%]	20	44	34
	20	τ	[MPa]	4.34	6.19	3.42
		s	[MPa]	1.33	1.22	0.95
		CV	[%]	31	20	28

identical average shear strength (9.84 MPa) was achieved at the test temperature of −5 °C and with timber samples with 10% moisture content. The lowest average shear strength (3.42 MPa) was obtained at the test temperature of 50 °C and with timber samples with 20% moisture content. An identical average shear strength (3.63 MPa) was achieved at the test temperature of −5 °C and with timber samples with 5% moisture content.

Although the lowest average shear strengths resulted from the extreme environmental conditions (lowest temperature with lowest moisture content and highest temperature with highest moisture content), the highest average shear strengths also resulted from the environmental condition where one environmental condition was extreme (lowest timber moisture content or lowest temperature). Fig. 8 offers an insight into the impact of different environmental conditions on the average shear strength. It can be seen how the combination of the studied environmental conditions (test temperature and timber moisture content) affected the shear strength.

Despite the fact that the glass strength is dependent on humidity, temperature and load duration, as Charles [21] says, this is a rather long term behaviour characteristic, at least compared to the short load

duration of the performed shear tests (approximately 1 min). It might, therefore, seem irrelevant to consider this effect in this study, but it should be noted that joints at −5 °C and 5% moisture, which most frequently failed due to "in-plane glass failure", showed lower shear strength values than at other conditions, where glass failure occurred.

The detailed results in the appendix (Appendix B. Individual shear specimen results) also show that 61 out of 63 shear specimens reached a shear strength equal or higher than the shear strength of timber class C24 (2.4 MPa). The shear strength parallel to the grain value for clear wood specimens of Norway spruce provided by Lavers [16] is equal to 9.8 MPa, which is of the same order as the maximum shear strength from the performed tests (12.19 MPa, see Appendix B. Individual shear specimen results). The actual timber rupture most likely happened due to a combination of shear parallel to the grain and tension perpendicular to the grain. As the Norway spruce tensile strength parallel to the grain is lower than the shear strength, this might be the reason for the shear strength values obtained from the shear specimen with failure type 1 (timber failure), which were considerably lower than the shear strength values parallel to the grain for clear wood specimens of Norway spruce.

Due to the various failure type combinations and the unknown sequence of failure types in a failure type combination, it is difficult to isolate the impact of the unfavourable failure types 2 (adhesive failure on glass) and 3 (adhesive failure) on the joint. If for example SSD N19 is considered, where pure failure type 2 (adhesion on glass failure) happened, it seems that the unfavourable failure type did not negatively impact the shear strength. The shear strength for SSD N19 was 10.42 MPa and the average shear strength for the corresponding environmental conditions was 9.84 MPa. For SSD V13, V14 and N12-14 on the contrary, it is clear that the joint shear strength was limited with the failure types 2 and 3, as failure type 3 was also the most frequent failure type of the corresponding environmental conditions.

As shown in Table 3, the coefficients of variation (CV) for the shear specimen shear strengths (τ) reach from 17% to 44%. Regarding the fact that the most frequent failure type was timber failure, it is worth to mention that Kretschmann [22] reports similar coefficients of variation (14%–34%) for mechanical properties of clear wood for various species. Considering the fact that the highest average shear strength (9.89 MPa) was observed at the same environmental conditions as the lowest coefficient of variation (17%), it might be concluded that these environmental conditions present the ideal environmental conditions for the considered timber-glass bonds.

3.2. Load-displacement curves

The testing device configuration used in this study was not ideal for studying shear specimen strains as the displacement results are cross-head movement recordings, which means that the recorded displacement is a sum of the shear specimen deformation, shear tool deformation and the universal testing machine compliance. Based on the assumption that the change in behaviour, from linear to nonlinear, is mostly the result of the epoxy resin reaction to different environmental conditions, it nonetheless offered an insight into the load-displacement behaviour. The load-displacement curves are given in Fig. 9 and have the same scale for better comparison. Although a preload was applied, the load-displacement curves for all environmental conditions had an initial part of stiffening (enlargement of the slopes of the curves), which varied from specimen to specimen. This happened due to the size tolerance for the shear specimens and due to some small irregularities of the shear specimen geometry. Some of the load-displacement curves (for example Fig. 9 a) also had some discontinuities, which happened due to the combination of different failure types. All specimen tests ended with an abrupt decrease of the test load, which indicates a generally abrupt energy release.

After the initial stiffening zone, the load-displacement curves showed almost linear behaviour, with the exception for the
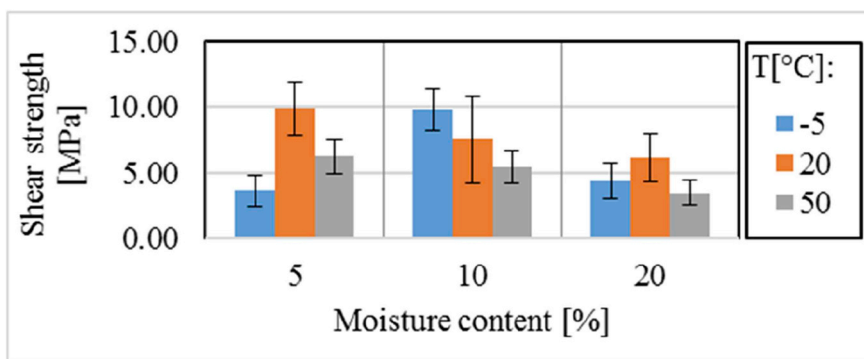
Fig. 8. Average shear strength of the shear specimens in relation to different test temperatures and timber moisture contents (with error bars representing standard deviation).

environmental conditions with a temperature of 50 °C with 10% and 20% timber sample moisture contents, where the curves were nonlinear in the final part. For the latter, the shear test continued even after the maximum load was reached. This might be due to the exceeded glass transition temperature, which is 43.6 °C as reported by Juvandes et al. [23], who determined it with the DSC method (Differential Scanning
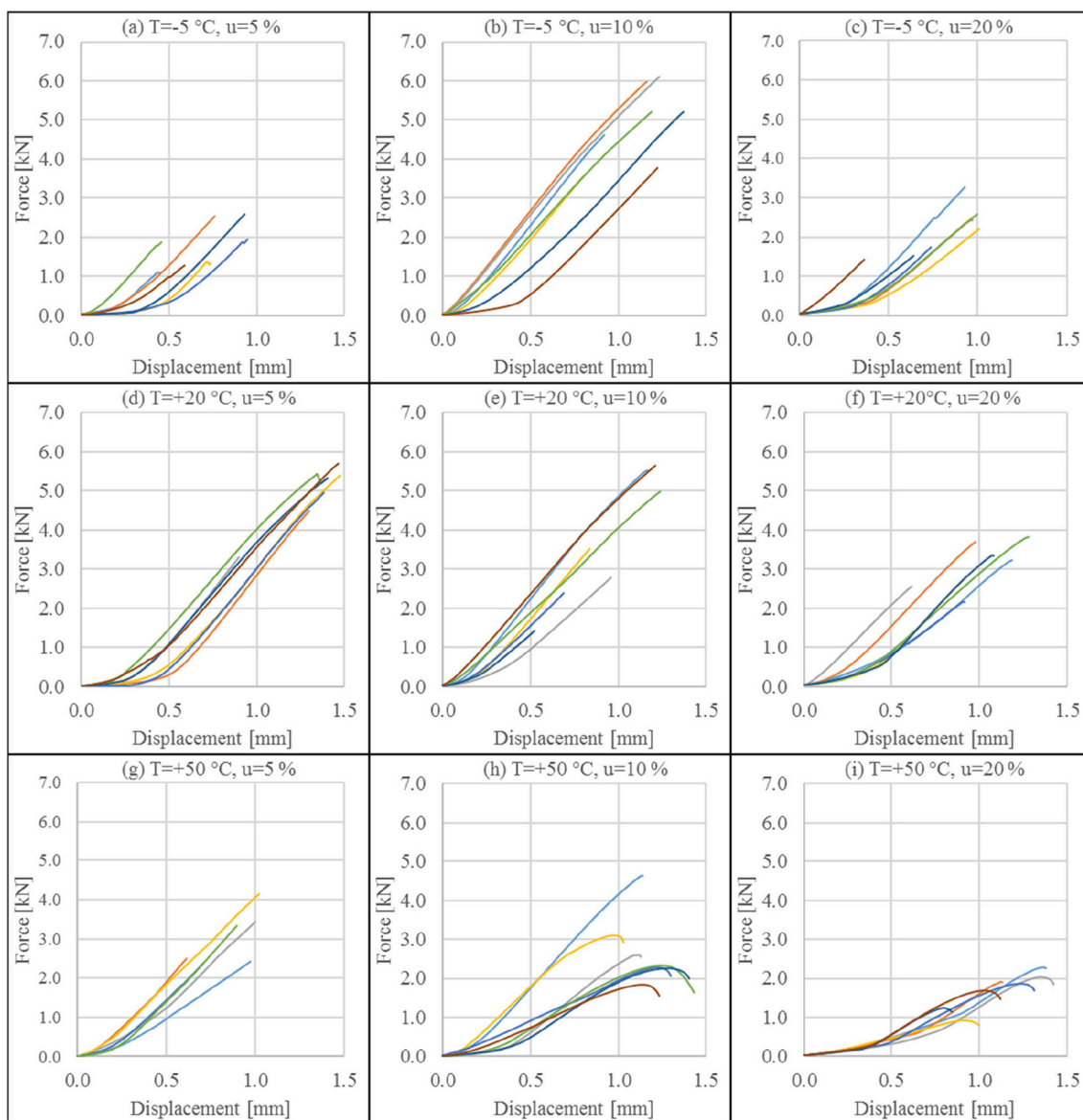
Fig. 9. Load-displacement curves for the shear specimens and for different environmental conditions (T – temperature during the test, u – moisture content of the timber samples). Displacement was measured by piston movement.

Calorimetry) and who cured the epoxy resin at natural environment temperature in the laboratory (T = 20 °C). According to the epoxy resin producer's description MAPEI [19], the glass transition temperature is higher than 40 °C. However, the nonlinearities in the final part of the load-displacement curves were not discovered for the environmental conditions with a test temperature of 50 °C and 5% timber moisture content. This indicates that the glass transition temperature of the used epoxy resin is influenced by the humidity conditions during the curing phase: a low humidity induces a higher glass transition temperature. This is in line with the observations made by DeIasi and Whiteside [24] who experimentally determined the glass transition temperatures of a number of epoxy resins for different curing phase humidity conditions and achieved good agreement with the theoretical curve for the effect of a diluent (in this case moisture) upon the glass transition temperature of a polymer derived by Kelley and Bueche [25]. Moreover, based on own experiments and on different literature, Ghiassi et al. [26] state that the degradation of epoxy resins due to water absorption can result in up to 45% lower elastic modulus values and up to 32% lower tensile strength values. Frigione et al. [27] suggest that the water absorbed by the epoxy adhesive acts as a plasticizer, which also lowers the glass transition temperature. Long exposure to a wet environment can also cause hydrolytic reactions which result in degradation of the adhesive (as stated by Kajorncheappunngam et al. [28]). Although, the shear specimen exposure time of only 7 days (as employed in this paper) is too short for the degradation processes to start. It is also known that epoxy adhesives become more ductile with increasing temperatures, resulting in lower strength and a lower elastic modulus and on the contrary, epoxy adhesives become more brittle at low temperatures, resulting in a higher strength and a higher elastic modulus, as shown for example in Na's et al. study [29]. However, as shown by Adams [30], the variation of strength of single lap shear joints is the result of the combination of the mismatch of the adherents or adhesive contraction and the stress/strain properties of the adhesives at different temperatures, which is in line with the shear strength results of the shear specimen in Fig. 8 and the observation of the environmental condition combination (test temperature and timber moisture content) affecting the shear strength.

3.3. Failure types

The shear specimen had 5 different failure types, which are presented in

Table 4. However, the actual failure was rarely in the form of a single failure type but was rather a combination of different failure types and it was impossible to determine the sequence of the failure types of an actual failure (combination) with the naked eye. The actual failures (failure type combinations) for each shear specimen are given in the appendix (Appendix A. Failure type combinations). From Table 5, it can be seen that the most frequent failure type was timber failure, with the exception for the environmental conditions with a temperature of 50 °C with 10% and 20% timber sample moisture contents, where the most frequent failure type was adhesive failure, and with the exception for the environmental conditions with a temperature of −5 °C with 5% timber sample moisture content, where the most frequent failure type was in plane glass failure. Although failure type 4 (out of plane glass failure) was not an interesting failure type for our study, as the glass crack happened outside of the bonding area and it was not related to a shear kind of failure, the strength results for this failure type were of similar magnitude as the results for other failure types.

Since timber failure was the most frequent failure type, the joint strength for the majority of the environmental conditions was basically subordinated to the timber strength. The impact of the timber moisture content on its mechanical properties is well known – a higher moisture content impacts the mechanical properties negatively. A somewhat less known behaviour is the impact of the temperature alone and combined with the timber moisture content. For a better understanding of the

Table 4
Failure types of the shear specimens.

Failure type	Description	Failure type photo
0	In-plane glass failure	
1	Timber failure	
2	Adhesive failure on glass	
3	Adhesive failure	
4	Out of plane glass failure	

Table 5
The most frequent failure types.

		T [°C]		
		−5	20	50
u [%]	5	0	1	1
	10	1	1	3
	20	1	1	3

joint behaviour, it is necessary to isolate the dependence of timber on the varying temperature. According to Desch and Dinwoodie [31], an important feature of timber is the relation between toughness and the combination of temperature and moisture content: toughness decreases with decreasing temperature at high moisture contents, while toughness increases with decreasing temperatures at low moisture contents. Desch and Dinwoodie [31] also state a rule of thumb which says that an increase of temperature by 1 °C decreases the timber strength and stiffness ultimate values by 1%. According to Gerhards [32], this effect is even greater for higher moisture contents. On the other hand, low temperatures and low moisture contents result in higher timber strength and stiffness, which is in line with the following observations: for joints at −5 °C temperature and 5% moisture content, the most frequent failure type was not timber failure anymore but (in-plane) glass failure.

Compared to the study of timber-glass adhesive joints performed by Blyberg et al. [11], in the presented study, a larger variety of the failure type combinations was observed. The reason might be the stiffness of the chosen adhesive, as epoxy resins are rigid adhesives. A stiffer adhesive probably blocks the deformation of the shear specimen in the sense of a better fit to the shear tools and consequently blocks the redistribution of the stresses.

Following the standpoint that a good joint is a joint where the failure happens outside of it, the failure types 2 (adhesive failure on glass) and 3 (adhesive failure) are the most unfavourable. Failure type 3 presents a pure epoxy resin cohesive behaviour and could, therefore, be studied by shear tests of solely the epoxy resin. Failure type 3, on the other hand, presents a mechanism of adhesion of the epoxy resin to the glass. The adhesion of the epoxy resin to timber obviously does not

Table 6
Number of occurrences of failure types 2 and 3.

		T [°C]					
		FT 2	FT 3	FT 2	FT 3	FT 2	FT 3
		−5		20		50	
u [%]	5	4	2	0	1	0	1
	10	2	1	0	3	3	6
	20	1	3	0	3	1	6

present a problem, as the shear specimen never failed in this way. The occurrence numbers of failure types 2 and 3 are given in Table 6. However, if only pure failure types were considered, failure type 2 happened twice, failure type 3 once, and the combination of failure types 2 and 3 happened thrice. The individual results for each SSD (shear specimen designation) are given in the appendix (Appendix B. Individual shear specimen results).

3.4. Annual ring width impact

As the majority of the shear specimens failed due to timber failure (failure type 1), a deeper look into the timber bonding interface was taken. The width of the annual rings on the bonding surface of the timber samples may be used as an indicator of the timber density – the lower the annual ring widths, the denser the timber, as Johansson [33] says. The density of timber is an important criterion when the penetration of some other material into the timber is important (for example, the penetration of wood preservatives). Furthermore, the mechanical interlocking theory is an important mechanism of adhesion and says that porous materials (with consequently rougher surfaces) improve the adhesive action. As the density is related to the porosity of a material (the denser the material, the less porous the material), the number of annual rings (an equivalent substitute for annual ring width) was determined for each sample (Appendix B. Individual shear specimen results). Although the adhesive failure on the timber surface never occurred, the penetration of the epoxy resin might influence the failure surface in the timber – the failure will most likely happen on a surface outside of the penetrated region. The deeper the penetration, the greater such a surface is. The results for the shear strengths of the specimens and the annual ring numbers were compared and the coefficients of determination (R^2) have been calculated (Table 7) for each environmental condition. It should be noted that the results for all shear specimens were considered, regardless of the failure type (combination) which was not necessarily timber failure. The highest correlation ($R^2 = 0.43$) was found for 20% moisture content and 20 ± 2 °C temperature; for other environmental conditions, the values were even lower. It may be concluded that only poor correlation has been found. The same was also done for the results from shear specimens whose failure type combination consisted of failure type 1 (timber failure), but the coefficients of determination were almost the same. As the timber samples were basically clear wood (timber parts free from defects), the microstructural properties must have influenced the timber bonding interface. As earlywood is weaker than latewood, the reason for the

Table 7
The coefficients of determination (R^2) of the relationship between the number of annual rings in the bonded area and measured shear strength (for different temperatures and moisture contents).

		T [°C]		
		−5	20	50
u [%]	5	0.21	0.00	0.01
	10	0.01	0.09	0.15
	20	0.14	0.43	0.28

Fig. 10. The ruptured timber surface (with latewood peaks).

missing correlation might also be the small surface area of the latewood regions compared to the whole annual ring width and that the timber failure is influenced by the failure of the earlywood regions. In addition, if a fixed ratio between the earlywood area and the latewood area per annual ring is assumed, the number of growth rings (or width of growth rings) does not affect the earlywood to latewood ratio of a given section.

Nevertheless, it was observed that the ruptured timber surfaces were uneven and that the latewood regions presented peaks of the uneven surfaces (Fig. 10). This might indicate that the penetration of the epoxy resin was deeper in the earlywood regions than in the latewood regions. The basis for this assumption is the fact that earlywood is less dense than latewood and consequently more permeable for the epoxy resin. According to Petric and Scukanec [34] more than 90% of Norway spruce wood volume consists of tracheids. The tracheid dimensions (diameter and wall thickness) therefore define the density of Norway spruce wood. According to Brändström's review study [35], the wall thickness of latewood tracheids is greater than the wall thickness of earlywood tracheids and the tracheid diameter of earlywood tracheids is greater than the tracheid diameter of latewood tracheids. The observed wavy pattern is also typical for the perpendicular to grain tensile fracture of wood when the fracture plane is inclined with respect on the growth rings or even when the tensile load acts in the radial direction, as shown by Gustafsson [36]. The observed fracture surface might therefore also be a consequence of tension perpendicular to the grain, as tensile stresses perpendicular to the bonding surface are also developed in lapped joints under shear loading (for an explanation see the work of Mays and Hutchinson [37]).

3.5. Finite element shear test simulation

Two different two-dimensional finite element analyses were performed for the studied shear specimens with the Autodesk® Inventor® Nastran 2020 software [38]. The purpose of performing two analyses was to determine the effect of the shear specimen rotation due to the slightly oversized shear tools as different shear test configurations have an important effect on the measured joint shear strength (see for example Serrano's study [15]). It is important to note that even if the shear tools were not oversized and there was almost no relative movement between the shear tools and the shear specimen, some rotation would still occur due to lateral shear tool displacement. Due to equilibrium conditions also forces which are perpendicular to the testing machine load are developed between the shear specimen and shear tools. To include this effect the shear specimen and shear tools were modelled (Fig. 11) in both analyses. By modelling the shear tools it was also achieved that the force action line was parallel to the bonding area and lying in the mid-plane of the adhesive layer (in the
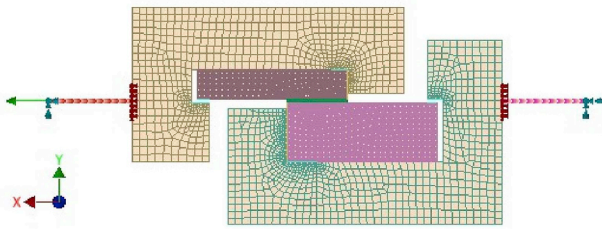
Fig. 11. The finite element model of the experiment.

initial state of undeformed geometry) for both analyses. Both analyses were geometrically nonlinear, basically meaning that the equilibrium equations have been written for the deformed rather than the original geometry and both analyses considered the changing contact conditions due to the rising load – the contacts between the shear tools and the shear specimen transferred only compressive forces and friction forces. The first analysis considered the contacts between the shear specimen and shear tools without clearance – this was achieved with defining offset contacts. This analysis was an approximation of a shear-compression test where the only specimen rotation results from the shear tools compliance and presents the ideal case of geometrical conformity of the shear tools and shear specimen. The second (nonlinear contact) analysis considered the actual clearance between the shear specimen and shear tools. The comparison of the results of the two analyses is an indicator of the oversized shear tools effect and the effect of shear specimen rotation inside the shear tools on the experimentally determined shear strengths. The coefficient of friction between timber and steel was set to 0.25 (according to the European standard EN 1995-1-1:2004) and the coefficient of friction between glass and steel was set to 0.5 (according to Buckley [39]).

The timber samples, glass samples and adhesive were modelled with quadrilateral parabolic shell elements. The element size in glass and timber was set to 0.5 mm, but close to the adhesive the element size was set to 0.25 mm. The adhesive element size was set to 0.25 mm, thus the adhesive was modelled with four layers of elements. The shear tools were modelled with triangular and quadrilateral parabolic shell elements with an edge size of 2.5 mm. At the contact regions the shear tool mesh was refined and given the edge size of 0.5 mm. The shear tool rods were modelled with beam elements. The material model for timber (Table 8) was orthotropic linear elastic with material parameters taken from Dahl and Malo [17]. Although it is specifically noted that the parameters are based on values available in the literature for different spruce species, the data should be appropriate as the comparison of the density and elastic modulus showed good agreement (see chapter 2.2.1). The epoxy resin was modelled with isotropic linear elastic material properties. The elastic modulus value was taken from Table 1 and the Poisson ratio from Table 2. The float glass was also modelled as an

isotropic linear elastic material with the elastic modulus equal to 70 GPa and the Poisson ratio equal to 0.23 (according to the draft European standard prEN 16612:2017) and so were the shear tools (E = 200 GPa and ν = 0.3). The chosen material properties correspond to a temperature of 20 °C and a timber moisture content of 10%. The load was set to 5000 N. The average shear stress in the adhesive equalled to 10 MPa and is similar to the maximum average shear strength determined from the experiments (9.89 MPa). In the sense of the load application, both analyses were of the shear-compression type. Note that the analyses presented here do not consider any bond damage behaviour as in the cohesive zone modelling (CZM) approach (for an example of the CZM approach for timber-glass bonds, see Piculin et al. [40]). Therefore, the analyses presented here are only an approximate presentation of the actual stress distribution and only valid for moderate load levels. Regarding the material nonlinearities, the timber material model presents the largest deviation from the actual behaviour (the compressive failure behaviour of timber is ductile). On the other hand, the actual material behaviour of float glass, steel and the epoxy resin (at 20 °C) is linear elastic for the stress levels in these analyses.

The unscaled deformed shapes of the two analyses can be seen in Fig. 12. For the analysis without clearance (Fig. 12 a), the displacements are relatively small compared to the analysis with clearance consideration, for which noticeable displacements can be seen (Fig. 12 b). Most of them are the result of the shear specimen rotation. From Fig. 12 b, it can be seen that the axis of the shear specimen rotation is in the timber sample in the vicinity of the adhesive. Fig. 12 a shows that the maximum displacement from the first analysis occurs in the shear tools, whereas Fig. 12 b shows that the maximum displacement from the second analysis occurs in the shear specimen. In both cases, the displacement is obviously a combination of displacements parallel and perpendicular to the force direction.

It must be noted that the experimental load-displacement results are crosshead displacement values from the universal testing machine and therefore also include the slip of the clamped shear tool parts (rods) and the testing machine compliance. In order to compare the force-displacement results of the finite element analysis with clearance consideration (actual test condition) and the experiments, an additional tensile test of the shear tool rod part was performed. The rod part was tested in tension up to 5000 N. The calculated compliance of the clamped rod length was subtracted from the ratio of the crosshead displacement and test force (in the sense of springs in series). Note that the axial compliance of the steel rods with 10 mm diameter with the length of 30 mm between the clamps is minimal and that the majority of the displacement results from testing machine compliance, slip of the rods inside the clamps and the deformability of the rods inside the clamps. The resulting stiffness (7088.85 N/mm, reciprocal of compliance) was then used to modify the displacement values at the force application point of the finite element analysis. The modified force-displacement curve of the finite element analysis with clearance consideration was plotted in the graph with the load-displacement results for the environmental conditions with a temperature of 20 °C and a timber moisture content of 10% (Fig. 13). The comparison of the finite element analysis results and the experimental results shows a relatively good agreement, especially the initial stiffening behaviour appears to be captured well.

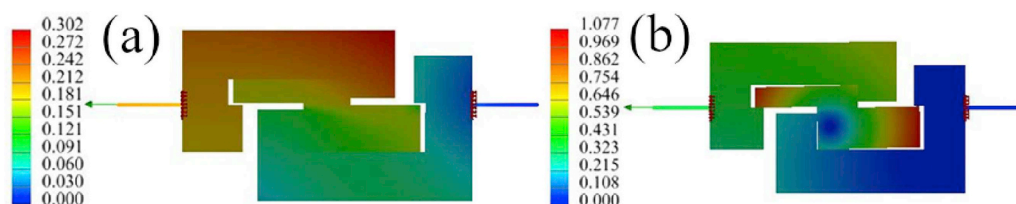The normal stress (perpendicular to the bond line) and shear stress

Table 8
Material parameters for modelling the timber samples (excerpted from Dahl and Malo [17]).

E_L [MPa]	E_T [MPa]	G_{LT} [MPa]	ν_{LT}
10991	435	693	0.48

Fig. 12. Deformed shape of the total displacement output vector (a: analysis without consideration of clearance, b: analysis with consideration of clearance) – total displacement legend in mm.
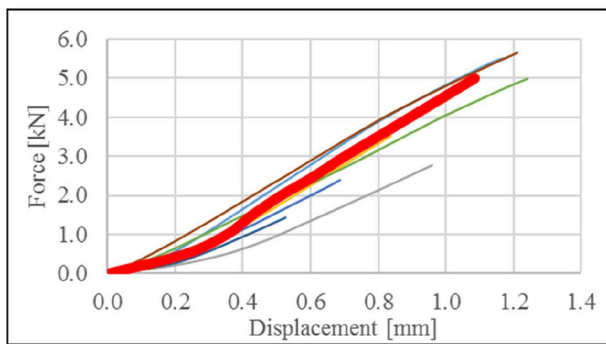
Fig. 13. Comparison of the finite element analysis load-displacement results (red thick line) and the experimental shear test load-displacement results (thin lines) for the environmental conditions with a temperature of 20 °C and a timber moisture content of 10%. (For interpretation of the references to colour in this figure legend, the reader is referred to the Web version of this article.)

(parallel to the bond line) distributions in the adhesive layer are given in Fig. 14. The adhesive mid-plane was defined as the stress path. Stress values at the finite element grid points were plotted. The shear stress distributions (Fig. 14-right) are identical and two peak stresses exist. The shear stress peaks are higher in the analysis without clearance consideration, which is expected as the shear specimen cannot rotate as much as if there is clearance (actual case) and the load stays nearly parallel to the adhesive layer. However, the deviation from the average shear stress (10 MPa) of the analysis with clearance consideration is less than the deviation of the analysis without clearance consideration. This means that the analysis with clearance consideration results in a higher normalised strength (the ratio of the joint strength to the local strength of the bond) if only linear material behaviour is considered.

The normal stress distributions (Fig. 14-left) of the two analyses are identical, but a nearer look on the results reveals that the analysis with clearance consideration produces higher tensile stresses (see Table 9). Based on the high tensile stresses in the vicinity of the timber sample edge and the low strength of the timber sample perpendicular to the

grain, it can be concluded that the finite element analyses confirmed that the failure of the shear specimen occurs at the timber sample edge. The comparison of the results of the two analyses shows that due to the oversized shear tools the shear specimen experiences higher tensile stresses and lower shear stresses as in the case when there is no clearance between the shear tools and shear specimen.

4. Conclusions

The shear specimen performance under different environmental conditions showed that the shear capacity of the timber-glass adhesive joint cannot be accurately predicted, without considering the temperature and timber moisture content simultaneously. The results showed that the shear strength is dependent on the combination of these two environmental conditions. Moreover, this dependence is not linear in the sense that the highest temperature and highest moisture content result in the lowest shear strength or vice versa. Considering the environmental condition combination with a temperature of 20 ± 2 °C and 10% timber moisture content as the typical or most frequent indoor conditions, it seems that timber is the weakest link in this joint and that the joint could be designed based only on the timber strength. Caution must be taken for other environmental condition combinations, especially the timber moisture content, which is an overall important factor when evaluating the condition of existing timber structures. At −5 °C and 50 °C, there was an increase in the number of occurrences of "adhesion failure on glass" and "adhesive failure". Based on the product data, the adhesive Adesilex PG1 should not be used at temperatures higher than 40 °C (the glass transition temperature), which is also what the results of the performed experiments suggest. Although, the load-displacement curves of the performed experiments confirm that the glass transition temperature can be manipulated (increased) to some extent when the moisture content in the timber is low (when the environment is sufficiently dry). In addition to the different moisture contents and temperatures, the timber density impact on the joint shear strength was controlled (indirectly by the annual ring width), but no dependence was found.
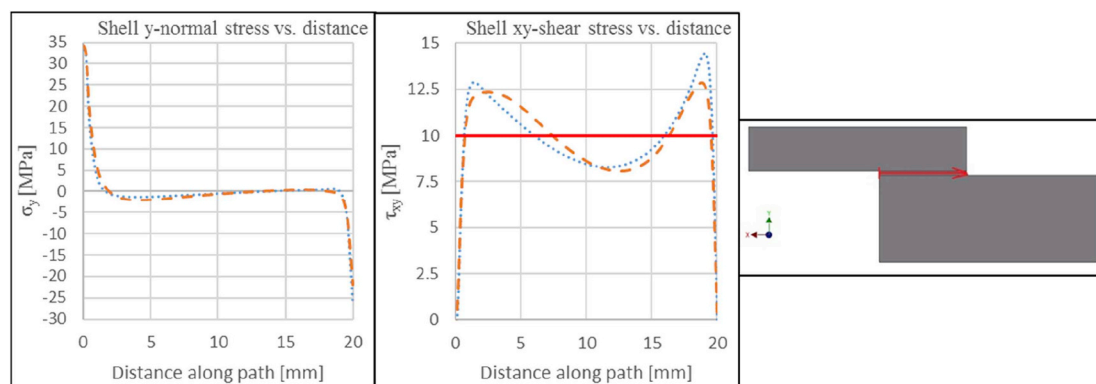

Fig. 14. Adhesive mid-plane normal stress distribution (perpendicular to the bond line), shear stress distribution (parallel to the bond line) and result path with direction for a temperature of 20 °C and timber moisture content of 10%; dashed line – results for the analysis with clearance consideration, dotted line – results for the analysis without clearance consideration, red solid line – the average shear stress (10 MPa). (For interpretation of the references to colour in this figure legend, the reader is referred to the Web version of this article.)

Table 9
Comparison of the maximum and minimum stresses from Fig. 14

	Stress component	Max. Stress Value [Mpa]	Corresponding distance along path [mm]	Min. Stress Value [Mpa]	Corresponding distance along path [mm]
Analysis with clearance consideration	σ_y	34.18	0.00	−22.05	20.00
	τ_{xy}	12.86	18.88	/	/
Analysis without clearance consideration	σ_y	33.20	0.00	−26.60	20.00
	τ_{xy}	14.41	19.13	/	/

The finite element simulations gave an insight of the stresses in the shear specimens and showed how rotation of the shear specimen due to the slightly oversized shear tools influenced the distribution of stresses in the shear specimen. The difference in the shear stress distribution seems to be of minor importance compared to the different tensile stress distributions, as the tensile strengths of glass and timber (perpendicular to the grain) are the weak points of those two materials. In this sense, the explored shear strength results are conservative.

Finally, the performed experiments indicate the suitability of the chosen rapid-setting thixotropic epoxy adhesive for bonding glass to timber and present the basis for future research on the application of glass as a strengthening element for existing timber structures.

Declarations of interest
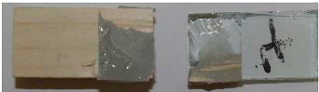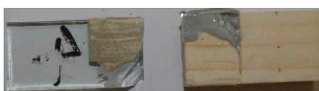
None.

Acknowledgements

Appendix A. Failure type combinations

Table A.1
Failure type combinations

Failure type combination	Failure type combination photo	Failure type combination	Failure type combination photo
0 + 1+2 + 3		1 + 4	
0 + 1		1 + 3	
0 + 1+3		1 + 2+3	
0 + 1+4		0 + 3	
0 + 2			

Appendix B. Individual shear specimen results

Table B.1
Individual shear specimen results

SSD	u [%]	T [°C]	F_{max} [N]	τ [MPa]	FTC	AR	SSD	u [%]	T [°C]	F_{max} [N]	τ [MPa]	FTC	AR
S1	5	−5	1113.34	2.23	0 + 1	13	N5	10	20	4971.63	9.94	0 + 1+3	10
S2	5	−5	2549.86	5.10	1 + 4	10	N6	10	20	1427.62	2.86	1 + 4	6
S3	5	−5	1369.44	2.74	0 + 1+2 + 3	4	N7	10	20	5638.39	11.28	0 + 1+3 + 4	10
S4	5	−5	1953.76	3.91	0 + 1+3	10	N8	10	50	4625.77	9.25	1	13
S5	5	−5	1860.83	3.72	0 + 2	9	N9	10	50	2611.63	5.22	0 + 1+3	20
S6	5	−5	2584.42	5.17	0 + 2	3	N10	10	50	3099.87	6.20	0 + 3	10
S7	5	−5	1275.01	2.55	0 + 2	13	N11	10	50	2294.23	4.59	0 + 1+3	13
S15	5	20	4493.07	8.99	4	21	N12	10	50	2333.41	4.67	2 + 3	7
S16	5	20	3309.03	6.62	1 + 4	7	N13	10	50	2253.96	4.51	2 + 3	7
S17	5	20	5414.19	10.83	1	9	N14	10	50	1837.56	3.68	2 + 3	3
S18	5	20	4967.29	9.93	0 + 1+4	15	V1	20	−5	3273.19	6.55	4	19
S19	5	20	5420.3	10.84	0 + 1	3	V2	20	−5	2442.05	4.88	1	19
S20	5	20	5317.2	10.63	1	4	V3	20	−5	2209.94	4.42	1 + 2+3	3
S21	5	20	5707.69	11.42	0 + 1+3	17	V4	20	−5	2590.4	5.18	1 + 3	9
S8	5	50	2421.64	4.84	1 + 4	6	V5	20	−5	1739.89	3.48	0 + 1+3	10
S9	5	50	2486.51	4.97	0 + 1	20	V6	20	−5	1509.39	3.02	4	17
S10	5	50	3438.05	6.88	0 + 1+3	7	V7	20	−5	1413.31	2.83	4	7
S11	5	50	4143.62	8.29	0 + 1+4	8	V15	20	20	3234.54	6.47	1	17
S12	5	50	2367.4	4.73	4	12	V16	20	20	3710.09	7.42	0 + 1+3	11
S13	5	50	3324.24	6.65	1 + 4	7	V17	20	20	2572.96	5.15	1 + 4	10
S14	5	50	3569.99	7.14	1	23	V18	20	20	2812.14	5.62	0 + 1+3	10
N15	10	−5	4625.66	9.25	1 + 4	16	V19	20	20	2162.41	4.32	1	9
N16	10	−5	5982.22	11.96	1	15	V20	20	20	3821.31	7.64	1	16
N17	10	−5	6093.33	12.19	1	15	V21	20	20	3354.1	6.71	0 + 1+3	17

Table B.1 (*continued*)

SSD	u [%]	T [°C]	F_{max} [N]	τ [MPa]	FTC	AR	SSD	u [%]	T [°C]	F_{max} [N]	τ [MPa]	FTC	AR
N18	10	−5	3546.47	7.09	1 + 4	8	V8	20	50	2293.76	4.59	1 + 3	12
N19	10	−5	5209.07	10.42	2	7	V9	20	50	1913.51	3.83	0 + 1+3	21
N20	10	−5	5201.18	10.40	1 + 2+3	9	V10	20	50	2034.7	4.07	0 + 3	9
N21	10	−5	3769.03	7.54	0 + 1+4	22	V11	20	50	924.53	1.85	1 + 3	6
N1	10	20	5515.74	11.03	1	20	V12	20	50	1864.86	3.73	0 + 3	16
N2	10	20	2782.46	5.56	0 + 1+3	7	V13	20	50	1250.8	2.50	2	9
N3	10	20	3532.42	7.06	1 + 4	20	V14	20	50	1686.53	3.37	3	10
N4	10	20	2395.09	4.79	1 + 4	17							

References

[1] Žegarac Leskovar V, Premrov M. Energy-efficient timber-glass houses. Springer; 2013.

[2] Blyberg L, Lang M, Lundstedt K, Schander M, Serrano E, Silfverhielm M, et al. Glass, timber and adhesive joints–innovative load bearing building components. Constr Build Mater 2014;55:470–8. 10/f24nvg.

[3] Rodacki K, Tekieli M, Furtak K. Contactless optical measurement methods for glass beams and composite timber-glass I-beams. Measurement 2019;134:662–72. 10/gf33nn.

[4] Premrov M, Zlatinek M, Štrukelj A. Experimental analysis of load-bearing timber-glass I-beam. Construction of Unique Buildings and Structures 2014;4:11–20.

[5] Ber B, Premrov M, Štrukelj A, Kuhta M. Experimental investigations of timber–glass composite wall panels. Constr Build Mater 2014;66:235–46.

[6] Cruz P, Pequeno J. Timber-glass composite structural panels: experimental studies & architectural applications. Challenging glass. Conference on architectural and structural applications of glass. 2008. p. 449–58. Delft.

[7] Ber B, Premrov M, Sustersic I, Dujic B. Innovative earthquake resistant timber-glass buildings. Nat Sci 2013;5:63. 10/gf4h97.

[8] Banea MD, da Silva LFM, Campilho RD. The effect of adhesive thickness on the mechanical behavior of a structural polyurethane adhesive. J Adhes 2015;91:331–46. 10/gf35xp.

[9] Campilho R, da Silva LF. Joint design in natural fiber composites. Natural fiber composites. CRC Press; 2015. p. 291–330.

[10] Cruz P, Pequeno J. Structural timber-glass adhesive bonding. Proceedings of challenging glass. 2008. p. 205–14.

[11] Blyberg L, Serrano E, Enquist B, Sterley M. Adhesive joints for structural timber/glass applications: experimental testing and evaluation methods. Int J Adhesion Adhes 2012;35:76–87.

[12] Vallee T, Grunwald C, Milchert L, Fecht S. Design and dimensioning of a complex timber-glass hybrid structure: the IFAM pedestrian bridge. Glass Structures & Engineering 2016;1:3–18.

[13] Buyuktaskin HAA, Yatagan MS, Soyoz GE, Tanacan L, Dilmaghani M. EXPERIMENTAL INVESTIGATION OF THE DURABILITY OF LOAD BEARING TIMBER-GLASS COMPOSITES UNDER THE EFFECTS OF ACCELERATED AGING. Journal of Green Building 2019;14:45–59. 10/gf4jcf.

[14] Nicklisch F. Ein Beitrag zum Einsatz von höherfesten Klebstoffen bei Holz-Glas-Verbundelementen [Application of high-modulus adhesives in load-bearing timber-glass-composite elements] PhD Thesis Technische Universität Dresden; 2016

[15] Serrano E. A numerical study of the shear-strength-predicting capabilities of test specimens for wood–adhesive bonds. Int J Adhesion Adhes 2004;24:23–35.

[16] Lavers GM. The strength properties of timber. Building Research Establishment vol. 60. London: HMSO; 1983.

[17] Dahl KB, Malo KA. Linear shear properties of spruce softwood. Wood Sci Technol 2009;43:499–525.

[18] Silvestru VA, Drass M, Englhardt O, Schneider J. Performance of a structural acrylic adhesive for linear glass-metal connections under shear and tensile loading. Int J Adhesion Adhes 2018;85:322–36.

[19] Adesilex MAPEI. PG1 Adesilex PG2 Two-component thixotropic epoxy adhesives for structural bonding 364/380-3-2016 (GB). 2016.

[20] Cerny M. Testing of composites for strengthening of RC structures. 2017. https://doi.org/10.15131/shef.data.5028089.v2.

[21] Charles RJ. Static fatigue of glass. II. J Appl Phys 1958;29:1554–60.

[22] Kretschmann D. Mechanical properties of wood. Wood handbook: wood as an engineering material: chapter 5 centennial ed general technical report FPL; GTR-190 Madison, WI: US Dept of Agriculture, Forest Service, Forest Products Laboratory; 2010. p. 51–546. 2010;190:5.1-5.46.

[23] Juvandes LFP, Costeira Silva P, Moreira J, Silva M, Alpalhão M. Thermal limits for external bonding repair method on structural surfaces exposed to the environment. Advanced composite materials in bridges and structures . 5th international conference: Winnipeg, Manitoba, Canada: September 22-24, 2008, Winnipeg, Manitoba, Canada: Canadian Society for Civil Engineering = Société canadienne de génie civil ; Printed by ISIS Canada Research Network. 2008.

[24] DeIasi R, Whiteside JB. Effect of moisture on epoxy resins and composites. Advanced composite materials—environmental effects. ASTM International; 1978.

[25] Kelley FN, Bueche F. Viscosity and glass temperature relations for polymer-diluent systems. J Polym Sci 1961;50:549–56. 10/fsspx4.

[26] Ghiassi B, Marcari G, Oliveira DV, Lourenço PB. Water degrading effects on the bond behavior in FRP-strengthened masonry. Compos B Eng 2013;54:11–9. 10/f48zbs.

[27] Frigione M, Lettieri M, Mecchi AM. Environmental effects on epoxy adhesives employed for restoration of historical buildings. J Mater Civ Eng 2006;18:715–22. 10/bzwdc9.

[28] Kajorncheappunngam S, Gupta RK, GangaRao HV. Effect of aging environment on degradation of glass-reinforced epoxy. J Compos Constr 2002;6:61–9. 10/bn4rmw.

[29] Na J, Mu W, Qin G, Tan W, Pu L. Effect of temperature on the mechanical properties of adhesively bonded basalt FRP-aluminum alloy joints in the automotive industry. Int J Adhesion Adhes 2018;85:138–48. 10/gf4hj2.

[30] Adams RD, Coppendale J, Mallick V, Al-Hamdan H. The effect of temperature on the strength of adhesive joints. Int J Adhesion Adhes 1992;12:185–90. 10/cdkqzn.

[31] Desch HE, Dinwoodie JM. Timber structure, properties, conversion and use. 1996. p. 7.

[32] Gerhards CC. Effect of moisture content and temperature on the mechanical properties of wood: an analysis of immediate effects. Wood Fiber 1982;14:4–36.

[33] Johansson C-J. Thelandersson S, Larsen H, editors. Grading of timber with respect to mechanical properties. vol. 2003. Wiley: Timber Engineering; 2003. p. 23–43.

[34] Petric B, Scukanec V. Volume percentage of tissues in wood of conifers grown in Yugoslavia. IAWA Bull Int Assoc Wood Anat; 1973.

[35] Brändström J. Micro-and ultrastructural aspects of Norway spruce tracheids: a review. IAWA J 2001;22:333–53. 10/gf23wn.

[36] Gustafsson PJ. Thelandersson S, Larsen H, editors. Fracture perpendicular to grain - structural applications. vol. 2003. Wiley: Timber Engineering; 2003. p. 103–30.

[37] Mays GC, Hutchinson AR. Adhesives in civil engineering. Cambridge University Press; 2005.

[38] Autodesk® Inventor® nastran version 2020.0.0.138. Autodesk®; 2019.

[39] Buckley DH. Friction behavior of glass and metals in contact with glass in various environments. NASA; 1973.

[40] Piculin S, Nicklisch F, Brank B. Numerical and experimental tests on adhesive bond behaviour in timber-glass walls. Int J Adhesion Adhes 2016;70:204–17.